Journal of Applied Polymer Science

Preparation of Composites of Liquid-Crystalline Matrix of Poly(*p*-phenylene-sulfoterephthalamide) and $CaCO_3$ by *In Situ* Mineralization

Takashi Nishio, Yuka Tanaka, Kensuke Naka
Department of Chemistry and Materials Technology, Graduate School of Science and Technology, Kyoto Institute of Technology, Goshokaido-cho, Matsugasaki, Sakyo-ku Kyoto 606-8585, Japan
Correspondence to: K. Naka (E-mail: kenaka@kit.ac.jp)

ABSTRACT: Liquid-crystalline (LC) hydrogels were obtained from an aqueous solution of poly(*p*-phenylene-sulfoterephthalamide) (PPST) by the addition of calcium ions (Ca^{2+}). The critical hydrogel formation ratio of Ca^{2+} to the sulfonic acid group in PPST ($^{crt}R_{Ca} = [Ca^{2+}]/[\text{-}SO_3^-]$) depended on the concentration of PPST, and was independent of the molecular weight of PPST. When the LC hydrogel was prepared at a concentration of 0.5 wt % and $^{crt}R_{Ca} = 0.6$, and was exposed to ammonium carbonate vapor for 96 h, all Ca^{2+} in the LC hydrogel were converted into calcite crystals. The alternate soaking process for the LC hydrogel induced the formation of two mesocrystal morphologies on and in the Ca^{2+} cross-linked LC hydrogel. Plate-like calcite mesocrystals grew at the hydrogel/solution interface and cubic mesocrystals were present in the inner space of the hydrogel, thus composites with some ordered structures of LC matrix and $CaCO_3$ have been prepared through *in situ* mineralization. © 2014 Wiley Periodicals, Inc. J. Appl. Polym. Sci. **2015**, *132*, 41455.

KEYWORDS: composites; gels; liquid crystals

Received 18 June 2014; accepted 25 August 2014
DOI: 10.1002/app.41455

INTRODUCTION

Natural composite materials produced by living organisms such as teeth, bone, nacre (mother of pearl), and egg shells have attracted significant interest over the last few decades because such materials seem to provide new pathways for producing light-weight materials with excellent mechanical properties.[1–23] Among them, the construction of calcium carbonate ($CaCO_3$) composite materials with controlled mineralization, analogous to those produced by nature, is a current interest for both organic and inorganic material chemists to understand the mechanism behind natural biomineralization processes as well as to identify novel industrial and technological applications.[1,5–8] Several remarkable imitations of hierarchical structures or well-ordered structures of $CaCO_3$ have been reported.[17,21–23] In these studies, organic gel-like matrices extracted from living organisms were used as the template for the mineralization.[17,21–23] Although synthetic polymer hydrogels were used as the matrix for the crystallization of $CaCO_3$, no ordered structure was obtained.[12–16,18,24]

Liquid-crystalline (LC) hydrogels have gained attention as a new class of soft materials inspired by tissues such as cartilage, muscle, and eye balls, which are endowed with excellent mechanical properties owing to its aligned structures.[25–33] However, most LC hydrogels which are physically cross-linked lack a well-ordered structure and have weak mechanical strength. Recently, the LC hydrogel based on semi-rigid aromatic polyelectrolytes has appeared as one of the interesting materials to overcome these drawbacks. For instance, a LC hydrogel based on poly(2,2′-disulfonyl-4,4′-benzidine terephthalamide) (PBDT) was prepared by the uniaxial diffusion of Ca^{2+} into an aqueous solution of PBDT, and the obtained LC hydrogel showed unique mechanical properties.[27,28] Recently, Viale et al. synthesized a sulfonated polyamide, poly(*p*-phenylene-sulfoterephthalamide) (PPST) (Chart 1), and studied its behavior in solution.[34–39] PPST shows a LC phase even at 0.5 wt % in water, suggesting the formation of a rod-like supramolecular structure with a high aspect ratio even in dilute solution.[36,37] The phase transition from an isotropic phase to a nematic phase occurs at a very low concentration, compared to that in a low-molecular-weight LC system, in which the same phase transition is observed at around 12 wt %.[37] Therefore, these semi-rigid aromatic LC hydrogels are attractive as templates for the self-aligned mineralization and composite preparation.

In this study, we investigated the LC hydrogel formation of PPST with calcium ions and employed the obtained LC hydrogel in template mineralization. We first studied the complexation

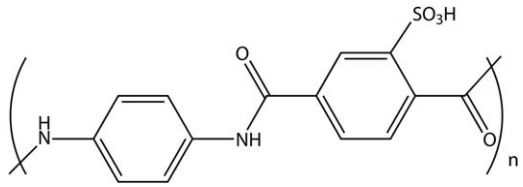

Chart 1. Structure of PPST.

behavior of PPST with Ca^{2+}, and found that LC hydrogel formation was independent of the molecular weight (MW) of PPST. An alternate soaking process (ASP), in which aqueous solutions of 1*M* calcium chloride ($CaCl_2$) and 1*M* ammonium carbonate [$(NH_4)_2CO_3$] were used as soaking solutions, led to the formation of a mineral rich layer-coated nematic LC hydrogel-$CaCO_3$ composite at the hydrogel/solution interface, while cubic mesocrystals grew in the inner space of the hydrogel.

EXPERIMENTAL

Materials

Ammonium carbonate, calcium chloride ($CaCl_2$), calcium hydroxide [$Ca(OH)_2$], and 1,4-phenylenediamine were obtained from Wako Pure Chemical Industries. Dowex-50wx4–200, lithium chloride (LiCl), and 1-methyl-2-pyrrolidinone (NMP) were purchased from Sigma-Aldrich Corporation. Triphenyl phosphite (TPP) was obtained from Tokyo Chemical Industry. Pyridine, and *p*-xylene-2-sulfonic acid were obtained from NACALAI TESQUE. Other solvents were of technical grade. All of them were used without further purification. 2-Sulfoterephthalic acid was synthesized by the oxidation of *p*-xylene-2-sulfonic acid according to a published procedure.[12]

Measurements

^{1}H NMR spectra in DMSO-d_6 were recorded on a 400MHz Bruker PDX-300. The MW of the synthesized polymers was measured by gel permeation chromatography (GPC) on a TOSOH 8020 GPC equipped with a TSK-GEL α-M column, calibrated with standard poly(styrene)s using *N,N*-dimethylformamide containing 10 m*M* LiBr as an eluent. A Nikon DS-L3 polarizing optical microscope (POM) was used to observe the LC structures of the samples. Solid phase analyses were performed using a scanning electron microscope (SEM; Keyence VE-8800), a field emission scanning microscope (FE-SEM; JEOL JSM-7600F) equipped with an energy dispersive X-ray spectrometer (EDX; Oxford Instruments X-max), an X-ray microdiffractometer (XRD; Rigaku Smartlab, emission source: Cu Kα), a Fourier transform infrared spectrometer (FT-IR; JASCO FT/IR-4100), and a thermogravimetric analyzer (TGA; TA Instruments TGA 2950) under air at a heating rate of 10°C/min.

Synthesis of PPST

PPST was synthesized according to a previous report with some modifications.[26] A typical polymerization was carried out as follows: 2-Sulfoterephthalic acid (1 g, 4.1 mmol), TPP (4.9 mL), LiCl (3.3 g), and pyridine (8.2 mL) were dissolved in NMP (30 mL). The solution was heated at 40°C for 15 min under N_2, and then 1,4-phenylenediamine (0.44 g, 4.1 mmol) dissolved in 10 mL of NMP was added under N_2. The reaction mixture was heated at 115°C for 4 h. The yellow, viscous solution was precipitated by slow addition to 1 L of vigorously stirred cold methanol. The precipitate was filtered and washed with methanol (500 mL) and diethyl ether (300 mL). The yellow/brown powder was dried under vacuum for 1 d. The as-prepared polymers contained cationic species such as lithium, pyridine, and phosphine derivatives. After complete dissolution of the sample (0.2 g) into technical-grade sulfuric acid (15 mL), Dowex resin (3 g) was added, and the solution was stirred for 24 h. The sulfuric phase was separated from the Dowex phase by using a glass fiber filter, and the polymer was precipitated by the slow addition of the sulfuric phase to vigorously stirred cold distilled water (350 mL). The precipitate was filtered and washed thoroughly with 0.1*M* sulfuric acid (100 mL) followed by methanol (200 mL). The polymer was dried under vacuum for 24 h. The overall yield was 32%. ^{1}H NMR (DMSO-d_6): δ 11.4 ppm (1H, s, NHCO), 10.7 ppm (1H, s, NHCO), 8.5 ppm (1H, s), and 8.1–7.7 ppm (6H, m).

Titration for Determining Critical Gel Formation Ratio

The critical gel formation ratio of calcium ions to the sulfonic acid groups in PPST ($^{crt}R_{Ca}$: $[Ca^{2+}]/[-SO_3^-]$) was determined as follows: 0.5 wt % $CaCl_2$ in water was added to 30 mL of an aqueous solution of PPST with stirring at room temperature. The concentration of PPST in the initial solution was varied from 0.25 wt % to 3.0 wt %. To avoid excess addition of $CaCl_2$ and subsequent collapse of the hydrogels, stirring was interrupted and the gelation was monitored by tilting the sample container. $^{crt}R_{Ca}$ at a certain C_p was estimated from the composition of the gelated mixture.

Preparation of Composites by Gas Diffusion Method (GDM)

A typical procedure was as follows: PPST hydrogels were prepared by the gradual addition of 0.17 wt % calcium hydroxide [$Ca(OH)_2$] aqueous solution (0.18 g) to 0.75 wt % PPST aqueous solution (0.30 g) under stirring. The concentration of PPST in the obtained hydrogel was 0.47 wt %. The hydrogel (150 mg), in a small plastic mold (volume 0.3 mL and diameter 7 mm), was placed in a chamber maintained at 45°C, and was exposed to ammonium carbonate vapor for 96 h.

Preparation of Composite by ASP

2.2 wt % PPST hydrogels were prepared from 3.0 wt % aqueous PPST-H solution (20 mL) with 0.5 wt % $CaCl_2$ in water (7.0 mL) ($R_{Ca} = 0.2$) using the same procedure described in the section entitled "Titration for determining the critical gel formation ratio." The hydrogel was cut in a cubic shape, ca., 5 mm on each side. The cubic hydrogels were sequentially immersed in 10 mL of 1*M* $CaCl_2$ in water at room temperature

Table I. Polymerization Results and Water Solubility of PPST

Designation	Reaction time of polymerization	M_W	M_w/M_n	Yield	Solubility in water[a]
PPST-H	240 min	50,000	3.1	32%	+++
PPST-M	170 min	28,000	3.1	25%	+++
PPST-L	90 min	9900	2.0	55%	–

[a] Polymer fraction is 0.5 wt %.
+++; transparent yellow solution, –; an opaque camel slurry.

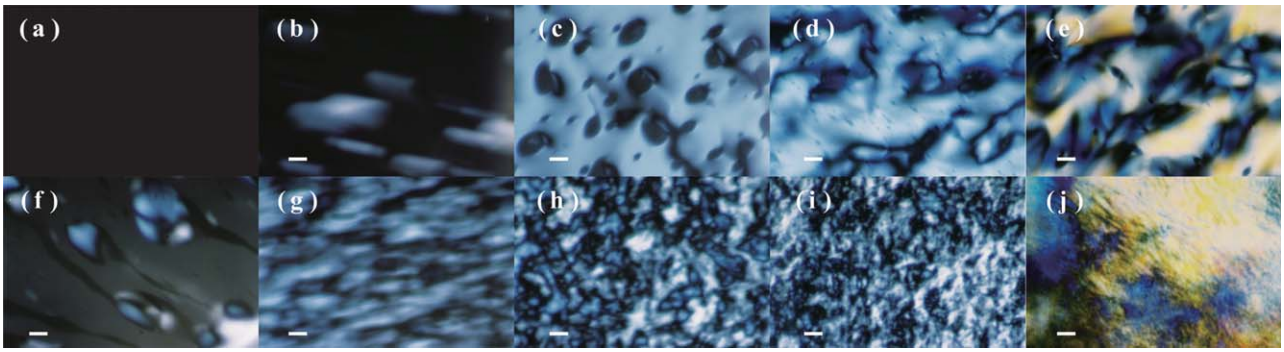

Figure 1. POM images of the PPST-M aqueous solutions at 0.5 wt % (a), 0.8 wt % (b), 2 wt % (c), 3 wt % (d), and 5 wt % (e), and the PPST-H aqueous solutions at 0.5 wt % (f), 0.8 wt % (g), 2 wt % (h), 3 wt % (i), and 5 wt % (j) (Scale bars, 25μm). [Color figure can be viewed in the online issue, which is available at wileyonlinelibrary.com.]

Table II. Critical Gel Formation Ratio ($^{crt}R_{Ca} = [Ca^{2+}]/[-SO_3^-]$)

	$^{crt}R_{Ca} = [Ca^{2+}]/[-SO_3^-]$ Concentration of PPST in the resultant hydrogel		
	0.2 wt %	0.5 wt %	2.2 wt %
PPST-H	1.4	0.6	0.2
PPST-M	-	0.6	-

for 1 day, rinsed with distilled water, immersed in 10 mL of 1*M* $(NH_4)_2CO_3$ in water at room temperature for 1 day, and rinsed again with distilled water. This serial process constituted one cycle, and five cycles were performed to prepare the $CaCO_3$ composites.

RESULTS AND DISCUSSION

Three PPST samples with different MWs were prepared by changing the polymerization time. Conditions and results of the polymerization are summarized in Table I. Although PPST-L was insoluble in water and gave an opaque camel slurry even after 12 h sonication, PPST-M and PPST-H were soluble in water and exhibited a lyotropic LC nature. An aqueous solution of PPST-M showed a biphasic texture at concentrations higher than 0.8 wt % [Figure 1(b)], and a schlieren texture was observed at a concentration above 3.0 wt % [Figure 1(d)]. 5.0 wt % PPST-M gave a colored nematic texture [Figure 1(e)]. Similar results were observed in the previous report.[36,37] In the case of an aqueous solution of PPST-H, a biphasic texture was observed even at a concentration of 0.5 wt % [Figure 1(f)], and the birefringence domains were larger than those of the PPST-M solution (Figure 1). These results indicated that a higher molar mass of PPST promoted LC behavior.

The addition of calcium ions to the aqueous solutions of PPST-H and PPST-M induced LC hydrogel formation. The critical gel formation ratios of $CaCl_2$ to the sulfonic acid groups of PPST-H and PPST-M ($^{crt}R_{Ca} = [Ca^{2+}]/[-SO_3^-]$) at 0.5 wt % were estimated by titration. The results are summarized in Table II. Interestingly, $^{crt}R_{Ca}$ of 0.6 was obtained for the PPST-H and PPST-M aqueous solutions when the concentration of PPST in the resultant hydrogels was 0.5 wt %. The PPST-H hydrogel was sliced at a thickness less than 1 mm and was placed between a cover glass and a microscope slide. The sample showed a blue birefringence under crossed Nicols condition of POM. On the other hand, the PPST-M hydrogel yielded an entirely black image under the same setting of POM observation for the PPST-H hydrogel, indicating the lack of an aligned LC structure. It was also found that higher concentrations of PPST required less calcium ions for the induction of gelation in the

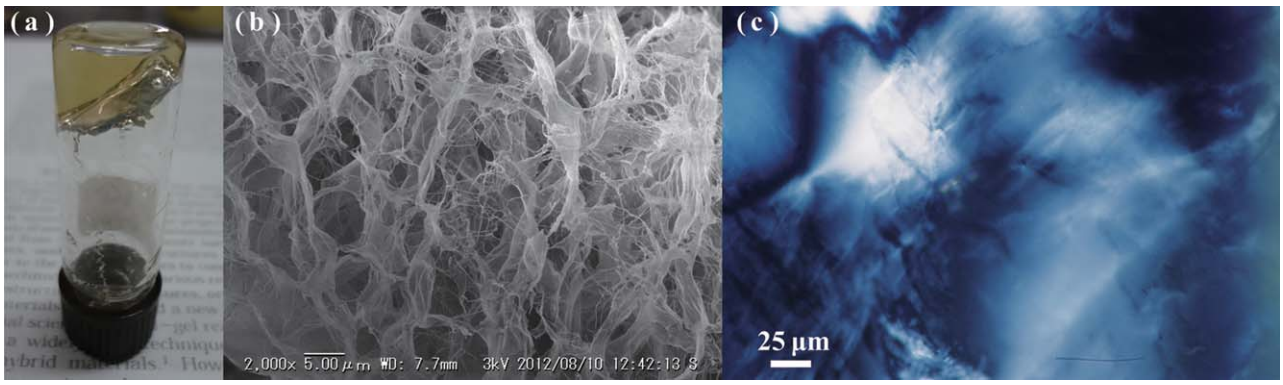

Figure 2. (a) Photo image, (b) SEM image of the freeze-dried specimen, and (c) POM image of the PPST-H hydrogel, in which the concentration of PPST-H was 0.5 wt %, prepared form the PPST-H aqueous solution with $Ca(OH)_2$. [Color figure can be viewed in the online issue, which is available at wileyonlinelibrary.com.]

Figure 3. (a) POM, (b) SEM images, and (c) mapping image of Ca on EDX of the self-standing film obtained from the PPST-H hydrogel by GDM and subsequent dehydration under vacuum. [Color figure can be viewed in the online issue, which is available at wileyonlinelibrary.com.]

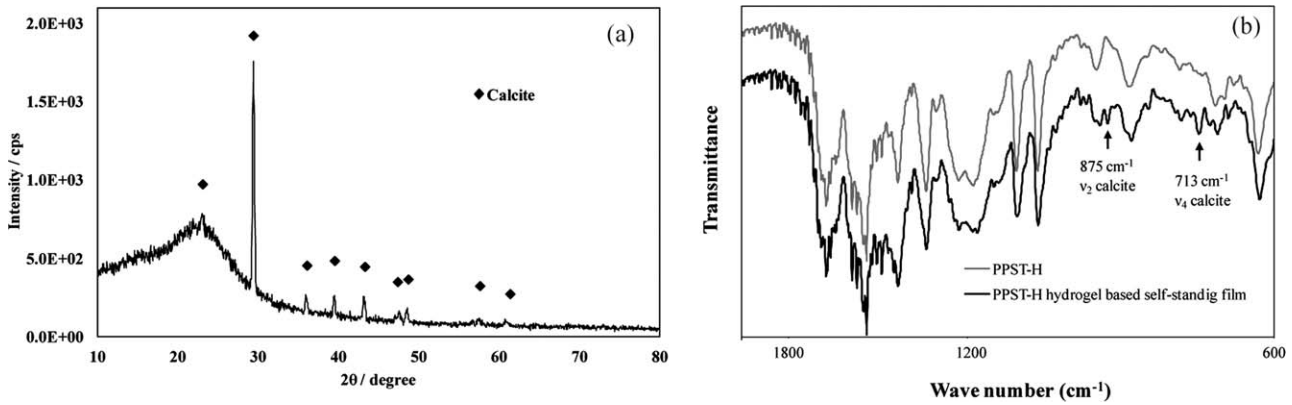

Figure 4. (a) XRD profile of the self-standing film obtained from the PPST-H hydrogel and (b) FT-IR spectra of PPST-H and the self-standing film obtained from the PPST-H hydrogel by GDM and subsequent dehydration under vacuum.

series of PPST-H aqueous solutions (Table II). No gel formation was observed with the addition of NaCl at the same ratio as that of calcium ions. These results suggested that the gelation occurred by calcium ion cross-linking, and the LC phase of PPST-H was maintained after the hydrogel formation. The critical gel formation ratio ($^{crt}R_{Ca}$) for an aqueous solution of PPST was studied by using 0.17 wt % $Ca(OH)_2$ in water, instead of the $CaCl_2$ solution to form the LC PPST-H hydrogel for mineralization in order to avoid the formation of ammonium carbonate during crystallization of $CaCO_3$ [Figure 2(a)]. The 0.5 wt % PPST-H aqueous solution gave the same critical gel formation ratio ($^{crt}R_{Ca} = 0.6$) as the $CaCl_2$ aqueous solution. The obtained PPST-H hydrogel showed a mixed fibrous and cellular interconnected pore structure [Figure 2(b)]. The PPST-H hydrogel obtained using the aqueous solution of $Ca(OH)_2$ also presented blue birefringence under the crossed Nicols condition of POM [Figure 2(c)]. According to the previous reports, the formation of LC phase occurs at such very low concentration, being a characteristic of supramolecular rod-like aggregates.[36–39]

The prepared PPST-H hydrogel was placed in a small plastic mold. Then, the mold was placed in a chamber at 45°C and was exposed to ammonium carbonate vapor for 96 h. Subsequently, a desiccated self-standing film was obtained by the vaporization of water. The obtained self-standing film was dehydrated under vacuum for 1 d.

POM and SEM images of the self-standing film obtained from the PPST-H hydrogel revealed that the film consisted of radially oriented and colored birefringent fibrous domains and cubic substances within the PPST matrix [Figure 3(a,b)]. EDX analysis of the film indicated that calcium elements were localized in the cubic substances [Figure 3(c,d)]. The XRD profile of the film showed a sharp and intense diffraction at $2\theta = 29°$, indicating calcite with a (104) flat face [Figure 4(a)]. The FT-IR analysis of the film showed absorptions at 713 cm^{-1} (ν_4, carbonate in-plane bending) and 875 cm^{-1} (ν_2, carbonate out-of-plane bending),

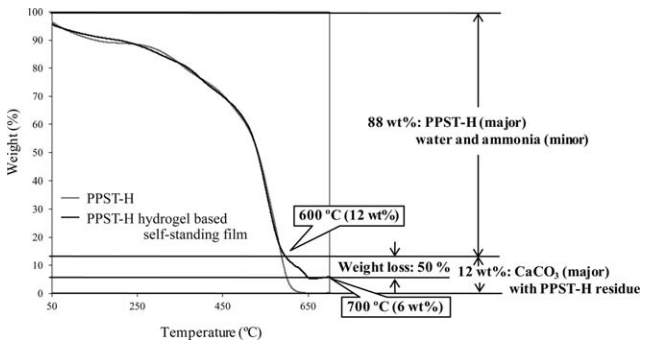

Figure 5. TGA profile of PPST-H and the self-standing film obtained from the PPST-H hydrogel by GDM and subsequent dehydration under vacuum.

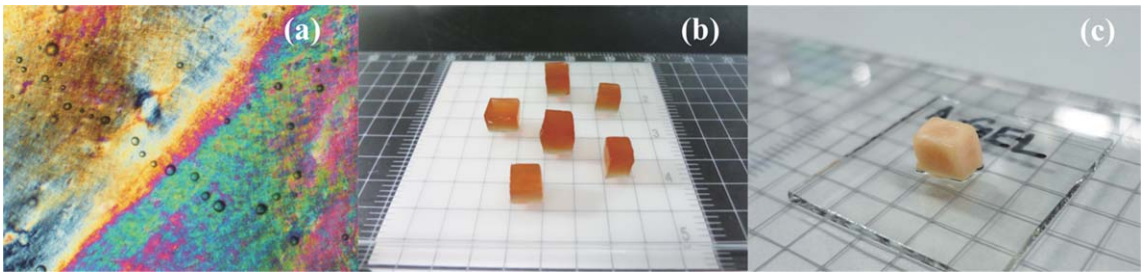

Figure 6. POM image (a) and photos of the 2.2 wt % PPST hydrogel (b) and the 2.2 wt % PPST hydrogel after five cycles of ASP (c). [Color figure can be viewed in the online issue, which is available at wileyonlinelibrary.com.]

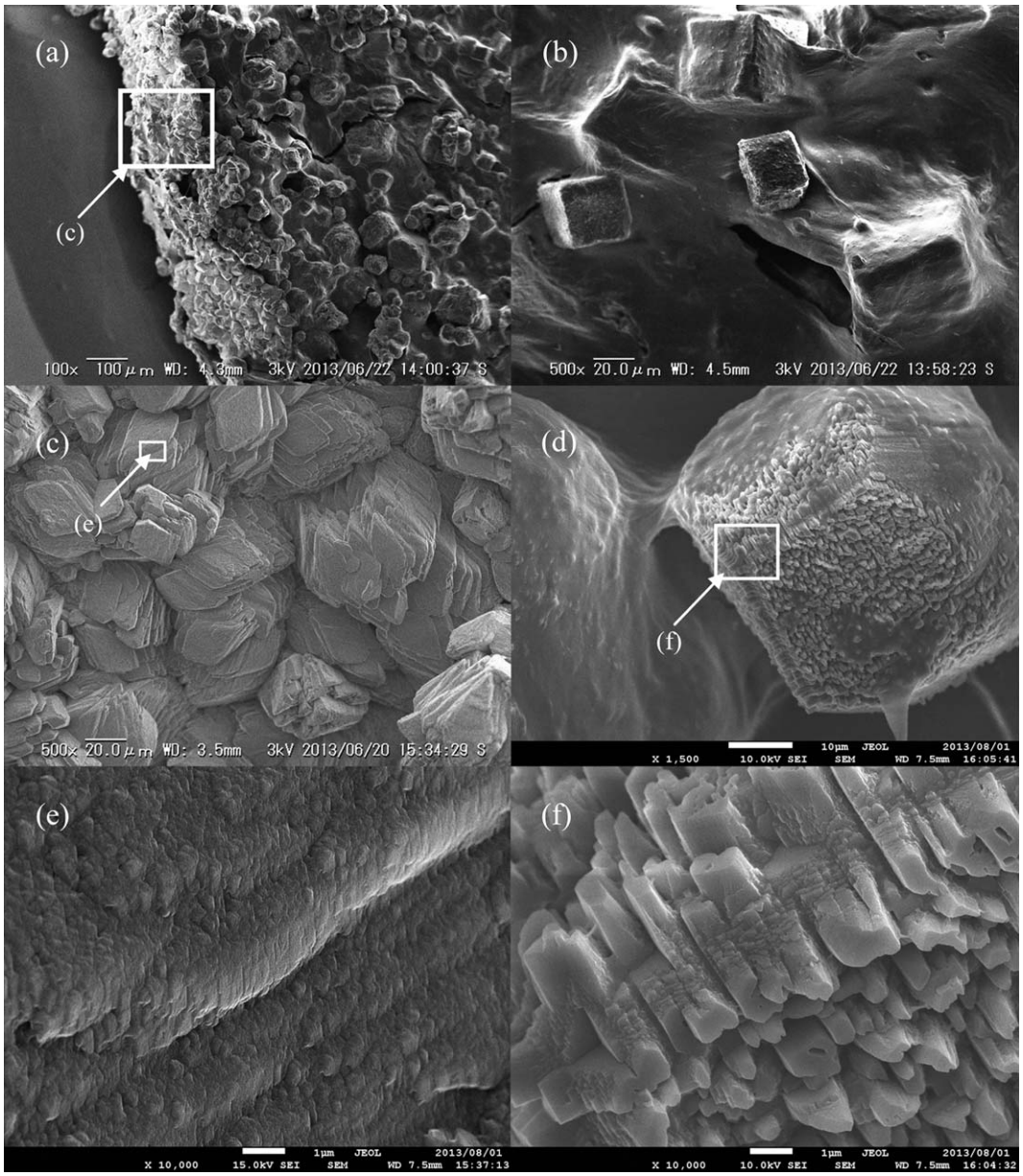

Figure 7. SEM images of the desiccated specimen of the 2.2 wt % PPST hydrogel after five cycles of ASP; (a) the cross-sectional region, (b) the inner space of the specimen, (c) the surface region corresponding to the area is indicated by the white frame in (a), (d) a magnified image of a cubic meso-crystal observed in the inner space of the specimen, (e) the area indicated by the white frame in (c) and analyzed by EDX, and (f) the area indicated by the white frame in (d) and analyzed by EDX.

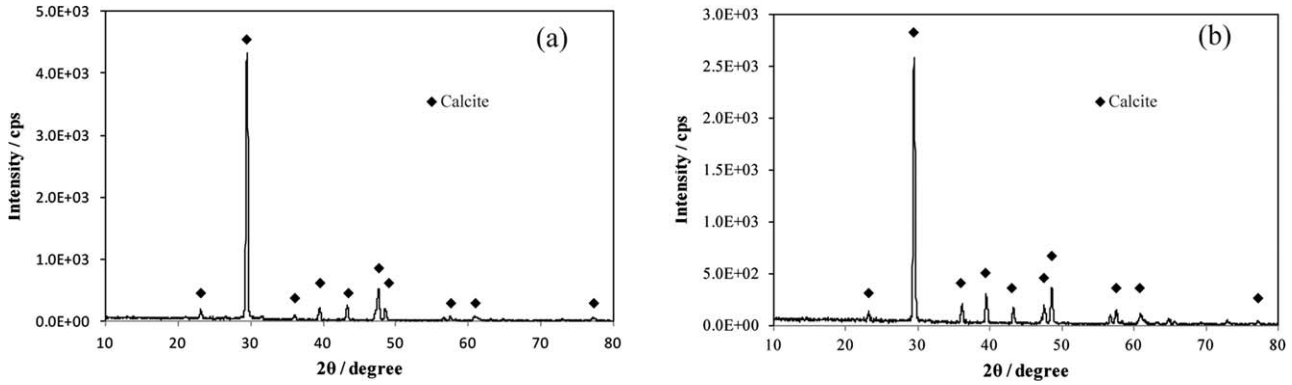

Figure 8. X-ray microdiffractometry profiles of the desiccated specimen of the 2.2 wt % PPST hydrogel after five cycles of ASP: an internal section of the hydrogel (a) and a superficial section of the hydrogel (b).

supporting the formation of calcite [Figure 4(b)]. These observations suggest that cubic shaped calcite crystals with diameters of several tens of μm were wrapped with fibrous PPST matrix.

The TGA analysis of PPST-H shows that a sharp weight loss occurs between 400°C and 600°C (Figure 5), and the TGA analysis of calcite shows that the decomposition of $CaCO_3$ releasing CO_2 starts from the temperature around 590°C and the corresponding weight loss at 700°C is ca. 44% of its initial weight. According to these results, the sharp weight loss of the obtained film between 400°C and 600°C was mainly due to the decomposition and combustion of PPST-H. The observed weight loss in the temperature range between 600°C and 700°C was 6 wt % and the remaining weight at 700°C was 6 wt % of the initial weight. Thus, the relative weight loss from 600°C and 700°C was calculated to about 50 wt % (Figure 5), which is in reasonable agreement with the theoretical loss of 44 wt % owing to the decarbonation from $CaCO_3$ to CaO. These results suggested that all Ca^{2+} in the hydrogel transformed to $CaCO_3$.

Next, an ASP was applied to prepare the PPST-$CaCO_3$ composites. In this process, 2.2 wt % PPST-H hydrogel was used, because increased concentrations of PPST accelerated the formation of $CaCO_3$. The 2.2 wt %-PPST hydrogel showed colored, nematic-like birefringence under the crossed Nicols condition of POM [Figure 6(a)], indicating the existence of rod-like supramolecular aggregates within the hydrogel structures. The as-prepared 2.2 wt %-PPST hydrogel was cut in a small cubic shape, ca., 5 mm on each side [Figure 6(b)]. Then the cubic 2.2 wt %-PPST hydrogels were soaked in aqueous solution of 1*M* $(NH_4)_2CO_3$ and 1*M* $CaCl_2$. In the course of five cycles of this serial process, the cubic hydrogel surface turned opaque and white [Figure 6(c)].

The SEM image of the cross-section of the desiccated 2.2 wt %-PPST hydrogel after five cycles of ASP exhibited a dense crystalline growth at the surface and sparse crystalline growth in the internal space of the specimen [Figure 7(a)]. The cubic morphology of the crystals in the internal space was similar to that of the self-standing film obtained by GDM [Figures 3(b) and 7(b)]. The major crystalline component in the internal space was identified as calcite by XRD [Figure 8(a)]. The magnified SEM image of the cubic crystals revealed mesocrystals consisting of aligned rod-like crystals (Figure 7(d,f)]. The incorporation of PPST in the cubic crystals was confirmed by EDX (Table III). Based on the atomic ratio of sulfur in the components as determined by EDX, the concentration of PPST incorporated in the cubic crystals was roughly 4 wt %.

The surface region of the 2.2 wt %-PPST hydrogel after five cycles of ASP was sliced to ca. 1-mm thickness and desiccated for further characterization. The SEM image revealed dense crystalline layers consisting of plate-like crystals (Figure 7(c)]. The magnified SEM image showed that the plate-like crystals were mesocrystals composed of aligned rod-like crystals [Figure 7(e)]. XRD analysis indicated that calcite was the dominant crystalline component of the plate-like crystals [Figure 8(b)]. In addition, EDX analysis suggested the incorporation of PPST in the plate-like crystals (Table III). Based on the atomic ratio of sulfur in the components as determined by EDX, the PPST content was roughly estimated to be 2 wt % in the plate-like mesocrystal phase.

Previous reports for $CaCO_3$ crystallization in hydrogels,[4,13] also described cubic $CaCO_3$ mesocrystals in hydrogels. The formation of cubic $CaCO_3$ mesocrystals can be explained as a result of the competition between the gel strength and the diffusion restrictions of reactants, i.e., Ca^{2+} or CO_3^{2-} (HCO_3^-), as well as

Table III. Element Compositions of the $CaCO_3$ Mesocrystals by EDX Analysis[a]

	Atomic ratio (%)					
Analyzed area	Ca	C	O	S	Cl	Total
Cubic mesocrystal [Fig. 7(f)]	18.30	19.88	61.40	0.26	0.16	100.00
Plate-like mesocrystal [Fig. 7(e)]	13.95	20.91	65.06	0.08	-	100.00

[a] Whole areas exhibited in the corresponding SEM images were analyzed.

the supersaturation, which depends on the chemical functional groups present in the matrix.[4,13] In the present case, cubic mesocrystals and plate-like crystals in the inside and surface of the gel, respectively, composed of aligned rod-like crystals were observed. At the gel/solution interface in ASP, the diffusion restrictions of reactants are negligible, whereas PPST hydrogel can work as a scaffold which provides nucleation sites; that is, the sulfonic acid group of PPST causes supersaturation. The different diffusion kinetics of reactants in and on the hydrogel matrix caused different morphologies of calcite crystals formed.

CONCLUSIONS

We prepared lyotropic LC hydrogels composed of PPST as an all aromatic semi-rigid polyaramide by the addition of calcium ions. The LC phase formation was dependent on the MW of PPST, so that higher MWs of PPST required lower concentrations of PPST for the LC phase formation. In addition, the critical gel formation ratio ($^{crt}R_{Ca}$) of PPST-H was dependent on the concentration of PPST-H: higher concentration of PPST-H led lower $^{crt}R_{Ca}$.

The GDM study of the LC hydrogel indicated that all calcium ions used for the cross-linking in the hydrogel were transformed to calcite. The ASP of the LC hydrogel formed a dense and mineral rich organic–inorganic composite layer on the surface of the LC hydrogel and cubic calcite formed in the inner space of the hydrogel. Both crystals were mesocrystals composed of aligned rod-like crystals.

The LC hydrogels of the all aromatic semi-rigid polymer acted as templates for the formation of $CaCO_3$ mesocrystals composed of aligned rod-like calcite crystals with the polymer. The present study provides a simple method for creating $CaCO_3$ polymer composites.

REFERENCES

1. Corni, I.; Harvey, T. J.; Wharton, J. A.; Stokes, K. R.; Walsh, F. C.; Wood, R. J. K. *Bioinspir. Biomim.* **2012**, *7*, 031001.
2. Naka, K.; Chujo, Y. *Chem. Mater.* **2001**, *13*, 3245.
3. Kato, T.; Sugawara, A.; Hosoda, N. *Adv. Mater.* **2002**, *14*, 869.
4. Meldrum, F. C.; Cölfen, H. *Chem. Rev.* **2008**, *108*, 4332.
5. Hosoda, N.; Sugawara, A.; Kato, T. *Macromolecules* **2003**, *36*, 6449.
6. Sugawara, A.; Ishii, T.; Kato, T. *Angew. Chem. Int. Ed.* **2003**, *42*, 5299.
7. Nishimura, T.; Ito, T.; Yamamoto, Y.; Yoshio, M.; Kato T. *Angew. Chem. Int. Ed.* **2008**, *47*, 2800.
8. Munro, N. H.; Green, D. W.; McGrath, K. M. *Chem. Commun.* **2013**, *49*, 3407.
9. Tang, Z.; Kotov, N. A.; Magonov, S.; Ozturk, B. *Nat. Mater* **2003**, *2*, 413.
10. Finnemore, A.; Cunha, P.; Shean, T.; Vignolini, S.; Guldin, S.; Oyen, M.; Steiner, U. *Nat. Commun.* **2012**, *3*, 1970/1.
11. Nakamura, S.; Naka, K. *Langmuir* **2013**, *29*, 15888.
12. Li, H.; Estroff, L. A. *J. Am. Chem. Soc.* **2007**, *129*, 5480.
13. Li, H.; Estroff, L. A. *Adv. Mater.* **2009**, *21*, 470.
14. Guvendiren, M.; Heiney, P. A.; Yang, S. *Macromolecules* **2009**, *42*, 6606.
15. Du, Z.; Lu, C.; Li, H.; Li, D. *Chin. J. Chem.* **2009**, *27*, 2237.
16. Zhong, C.; Chu, C. C. *J. Mater. Chem.* **2012**, *22*, 6080.
17. Yamamoto, Y.; Nishimura, T.; Saito, T.; Kato, T. *Polym. J.* **2010**, *42*, 583.
18. Asenath-Smith, E.; Li, H.; Keene, E. C.; She, Z. W.; Estroff, L. A. *Adv. Funct. Mater.* **2012**, *22*, 2891.
19. Schäffer, T. E.; Ionescu-Zanetti, C.; Proksch, R.; Fritz, M.; Walters, D. A.; Almqvist, N.; Zaremba, C. M.; Belcher, A. M.; Smith, B. L.; Stucky, G. D.; Morse, D. E.; Hansma, P. K. *Chem. Mater.* **1997**, *9*, 1731.
20. Smith, B. L.; Schäffer, T. E.; Viani, M.; Thompson, J. B.; Frederick, N. A.; Kindt, J.; Belcher, A.; Stucky, G. D.; Morse, D. E.; Hansma, P. K. *Nature* **1999**, *399*, 761.
21. Watabe, N.; Wilbur, K. M. *Nature* **1960**, *188*, 334.
22. Gehrke, N.; Nassif, N.; Pinna, N.; Antonietti,M.; Gupta, H. S.; Cölfen, H. *Chem. Mater.* **2005**, *17*, 6514.
23. Keene, E. C.; Evans, J. S.; Estroff, L. A. *Cryst. Growth. Des.* **2010**, *10*, 5169.
24. Kuang, M.; Wang, D.; Gao, M.; Hartmann, J.; Möhwald, H. *Chem. Mater.* **2005**, *17*, 656.
25. Haque, Md. A.; Kurokawa, T.; Gong, J. P. *Soft Matter* **2012**, *8*, 8008.
26. Wu, Z. L.; Kurokawa, T.; Sawada, D.; Hu, J.; Furukawa, H.; Gong, J. P. *Macromolecules* **2011**, *44*, 3535.
27. Wu, Z. L.; Kurokawa, T.; Kakugo, A.; Yang, W.; Furukawa, H.; Gong, J. P. *Macromolecules* **2011**, *44*, 3542.
28. Yabuuchi, K.; Rowan, A. E.; Nolte, R. J. M.; Kato, T. *Chem. Mater.* **2000**, *12*, 440.
29. Kato, T.; Mizoshita, N.; Kishimoto, K. *Angew. Chem., Int. Ed.* **2006**, *45*, 38.
30. Sangeetha, N. M.; Maitra, U. *Chem. Soc. Rev.* **2005**, *34*, 821.
31. Coppin, C. M.; Leavis, P. C. *Biophys. J.* **1992**, *63*, 794.
32. Tamm, E. R.; Lutjen-Drecoll, E. *Microsc. Res. Tech.* **1996**, *33*, 390.
33. Sanchez, C.; Arribart, H.; Giraud-Guille, M. M. *Nat. Mater.* **2005**, *4*, 277.
34. Viale, S.; Jager, W. F.; Picken, S. J. *Polymer* **2003**, *44*, 7843.
35. Mendes, E.; Viale, S.; Santin, O.; Heinrich, M.; Picken, S. J. *J. Appl. Crystallogr.* **2003**, *36*, 1000.
36. Viale, S.; Best, A. S.; Mendes, E; Jager, W. F.; Picken, S. J. *Chem. Commun.* **2004**, 1596.
37. Viale, S.; Li, N.; Schotman, A. H. M.; Best, A. S.; Picken, S. J. *Macromolecules* **2005**, *38*, 3647.
38. Sisbandini, C.; Every, H. A.; Viale, S.; Mendes, E.; Picken, S. J. *J. Polym. Sci., Part B: Polym. Phys.* **2007**, *45*, 666.
39. Every, H. A.; van der Ham, L.; Picken, S. J.; Mendes, E. *Soft Matter.* **2009**, *5*, 342.